



ELSEVIER

Soil Dynamics and Earthquake Engineering 23 (2003) 53–63

SOIL DYNAMICS
AND
EARTHQUAKE
ENGINEERING

www.elsevier.com/locate/soildyn

Seismic behavior of a post-tensioned integral bridge including soil–structure interaction (SSI)

Constantine Spyrakos^{a,*}, George Loannidis^b

^aLaboratory of Earthquake Engineering, Department of Civil Engineering, National Technical University of Athens, Polytechnic Campus Zografos, Athens 15700, Greece

^bPythagora 87, Thessaloniki, Greece

Abstract

Current practice usually pays little attention to the effect of soil–structure interaction (SSI) on seismic analysis and design of bridges. The objective of this research study is to assess the significance of SSI on the modal with geometric stiffness and seismic response of a bridge with integral abutments that has been constructed using a new bridge system technology. Emphasis is placed on integral abutment behavior, since abutments together with piers are the most critical elements in securing the integrity of bridge superstructures during earthquakes. Comparison is made between analytical results and field measurements in order to establish the accuracy of the superstructure–abutment model. Sensitivity studies are conducted to investigate the effects of foundation stiffness on the overall dynamic and seismic response of the new bridge system.

© 2002 Published by Elsevier Science Ltd.

Keywords: Bridge; Seismic analysis; Soil–structure interaction

1. Introduction

In order to perform a meaningful modal and seismic response analysis for many common types of bridges, an evaluation of the dynamic soil–structure interaction (SSI) effects of the foundation system for earthquake loading, is required. The significance of accounting for the effects of SSI on the design of bridges has also been experimentally verified, e.g. [1]. While the AASHTO specifications [2] and Eurocode 8 [3] make specific recommendations with respect to structural analysis and design of bridges for earthquake loading, they are less specific with respect to foundation analysis and design. In part this is attributed to the complexities that are associated with bridge foundation systems and the wide variety of soil types encountered in practice.

Ideally, earthquake response of bridges should be evaluated with a single direct analysis that models the whole system consisting of the superstructure, foundation and the soil mass. However, such an approach is beyond the ‘state of practice’ at the present time because of the complexity involved in modeling the foundation soil–system.

Instead SSI analyses are usually conducted using the substructure method that utilizes a two-step approach, e.g. Imbsen [4], Wolf [5], Antes and Spyrakos [6].

Spyrakos [7,8] has assessed the significance of SSI on the seismic response of short span bridges. The focus has been placed on pier behavior, since piers together with the abutments are the most critical elements in securing the integrity of bridge superstructures during earthquakes. His studies conclude that safer and more economical bridge designs can be obtained by properly accounting for SSI.

Crouse, Hushmand and Martin [9], have presented experimental and analytical studies to determine dynamic SSI characteristics of a single-span, prestressed-concrete bridge with monolithic abutments supported by spread footings. Using a three-dimensional (3D) finite element model of the bridge, with Winkler springs attached to the footings and abutment walls to represent SSI, they have been able to reproduce the experimentally determined natural frequencies, mode shapes and bridge response reasonably well.

Levine and Scott [10] have introduced a simplified method to determine rotational boundary stiffnesses that represent the foundation of a structure and its surrounding soil. A very simple 3D finite element beam model for the bridge is constructed, and the rotational stiffnesses are

* Corresponding author. Tel.: +30-1-699-0044; fax: +30-1-699-0044.
E-mail address: spyrakos@hol.gr (C. Spyrakos).

used to model the foundations. Simple one- and two-degree of freedom systems for preliminary seismic design of bridges are proposed in the textbook of Priestley et al. [11]. Design recommendations to account for SSI are also presented in the textbook of Spyrakos [12].

Saiidi and Douglas [13] have developed an inelastic bridge model that accounts for the nonlinear action at the pier to foundation connections. Comparison of the experimental and analytical results has shown that, by ignoring the foundation flexibility, an assumption made in bridge design, the lateral displacement at the deck center is underestimated by approximately 50%.

A simple analytical model has been developed by Wilson [14] to describe the stiffness of nonskew monolithic highway bridge abutments for seismic bridge analysis. The model uses six equivalent discrete spring stiffnesses for three translational and three rotational degrees-of-freedom of the abutment and accounts for the interaction of the abutment walls, pile foundations and soil.

An analytical method to estimate the elastic stiffness of columns with a parabolic flare at the top and translational and rotational foundation springs at the bottom has been presented by Maragakis [15]. Bridge columns with flare have been extensively used by bridge engineers in the design of highway bridges.

Elassaly et al. [16] and Cook et al. [17] have shown that the effects of local soil conditions and SSI substantially affect the seismic behavior of cable-stayed bridges.

A recent study by Karantzikis and Spyrakos [18] demonstrates the importance in accounting for soil–abutment interaction of integral bridges and develops an iterative design procedure of successive linear dynamic response analyses that considers the nonlinear behavior of the abutment caused by backfill soil yielding.

The effect of SSI of seismically isolated bridges has been studied in a recent publication of Vlassis and Spyrakos [19]. In their study the relative significance of SSI and base isolation is evaluated for a bridge system commonly used in practice.

In this paper the effect of dynamic SSI is studied for a new post-tensioned bridge system. The study examines the seismic response of the system based on the analytical model validated through in situ testing. Parametric studies are conducted to evaluate the response of the bridge system for various soil conditions.

2. Description of bridge system and analysis procedure

This section briefly describes the new post-tensioned bridge system constructed at East Logansport in West Virginia in late 1995. East Logansport Bridge consists of a 28.7 m clear span steel superstructure, with four 91-cm diameter galvanized steel tubes, as shown in Figs. 1 and 2,

made of 13-mm thick steel plate. Each tube is made up of three segments 6.1-m long connected with two segments approximately 5.3-m long. The superstructure is post-tensioned with twelve 3.5-cm diameter polycoated Dywidag rods, six for each pair of tubes. The deck consists of precast concrete panels 3.1-m long and 5.3-m wide, that simply rest on the steel tubes. A small number of shear studs is used to connect the panels to the tubes without providing composite slab-stringer action. A precast concrete barrier parapet is bolted to the deck.

Soil samples collected from four 5.5-m deep bareholes near the base of the abutment indicated that the soil below the bridge is mostly composed of medium hard rock. A primary advantage of the bridge superstructure is the ease of either placing or replacing the concrete deck, an advantage that allows for cost effective maintenance of the bridge system over conventional bridge systems.

East Logansport Bridge has been constructed with concrete abutments ($f'_c = 34.5$ MPa) that are cast monolithically with the superstructure acting as prop between the abutments. At the base of the East Logansport abutment wall a hinge is constructed to reduce the loads on the foundations of the abutments. The dimensions of the concrete abutments are shown in Fig. 3. For this type of abutments, longitudinal earthquake-induced inertia forces are transmitted directly from the superstructure to the soil behind the end diaphragm without having to pass through bearing devices. This kind of systems have performed well during earthquakes avoiding problems such as backwall and bearing damage associated with seat-type abutments and also reducing the lateral load taken by columns or shafts [11,20]. However, provision must be made for adequate passive resistance from the soil to avoid excessive displacement [3,18] and procedures to evaluate abutment stiffness are necessary to assess the natural frequencies of the superstructure. In several experimental studies for relatively short bridges (with spans shorter than 61 m), damping arising from soil–abutment interaction has been found to be very significant, as much as 15% of critical damping for the longitudinal mode of response [20].

Seismic design specifications and codes for highway bridges generally recommend that the effects of earthquake loading are evaluated using either an equivalent static load approach or a dynamic analysis [2,3,21]. They usually provide explanations on techniques suitable for static and dynamic modeling of the bridge superstructure and supporting columns and piers. There is, however, a significant lack of guidance on exactly how the boundary conditions and SSI at the abutments should be incorporated into the model. For various abutment configurations and soil conditions, a general form of abutment wall-backfill stiffness equation that considers passive resistance of soil is adopted in this work to estimate the longitudinal stiffness of the end-wall and the transverse stiffness of

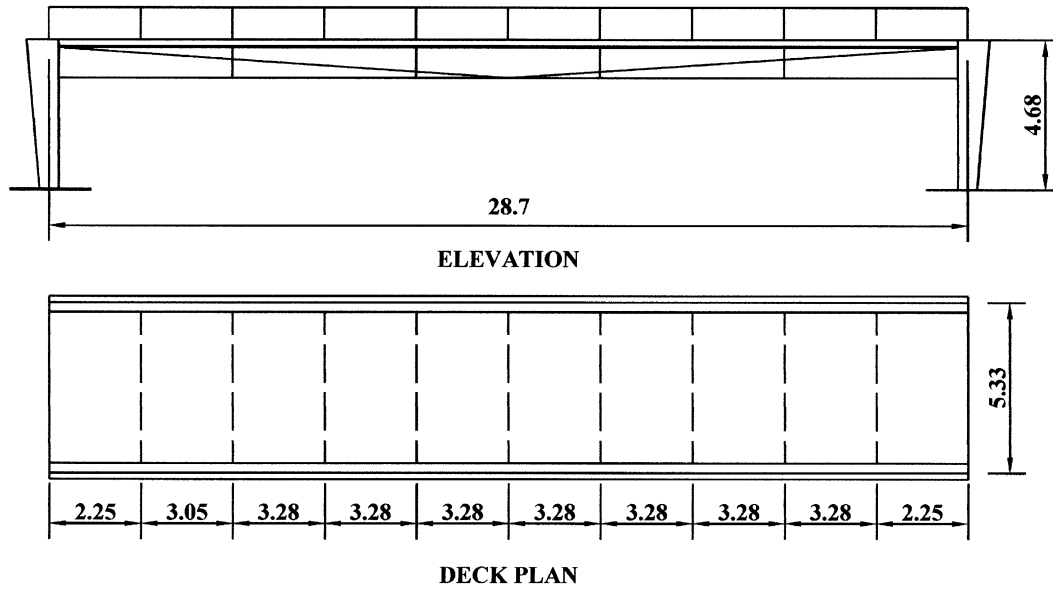


Fig. 1. Elevation and deck plan of the East Logansport Bridge.

the wing-wall [14], that is

$$K_s = \frac{E_s}{(1 - \nu^2)I} \quad (1)$$

where K_s is soil stiffness per unit wall width; E_s and ν are the Young’s modulus and the Poisson’s ratio, respectively, of the backfill soil; and I is a shape factor. Representative values of I are given in Table 1 [21].

Eq. (1) is used to evaluate vertical displacement of a uniformly loaded area resting on an elastic half-space, which is available in standard geotechnical references [22].

Evaluating soil stiffness as described above is just one possible approach to account for translational stiffness of end- and wing-walls. Other models [23,24], that have received widespread use to estimate foundation stiffness and are equally as convenient to use, could have also been adopted in this work.

Eq. (1) allows for input of site specific soil parameters and abutment wall configurations. As the length to height ratios for wing-walls are somewhat smaller than end-walls, Eq. (1) suggests a lower shape factor I , or a higher soil stiffness (K_s) for wing-walls as compared to end-walls.

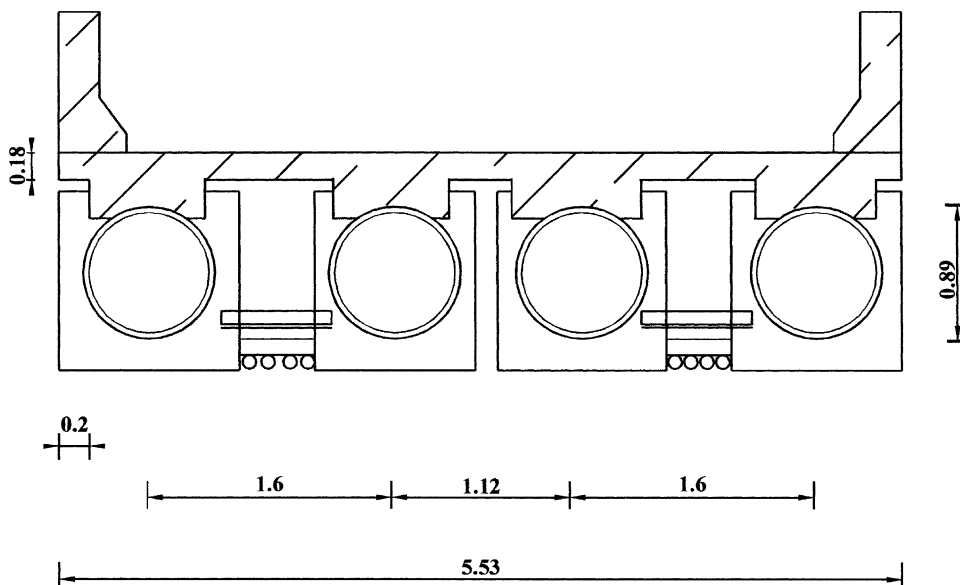


Fig. 2. Cross-section of the East Logansport Bridge.

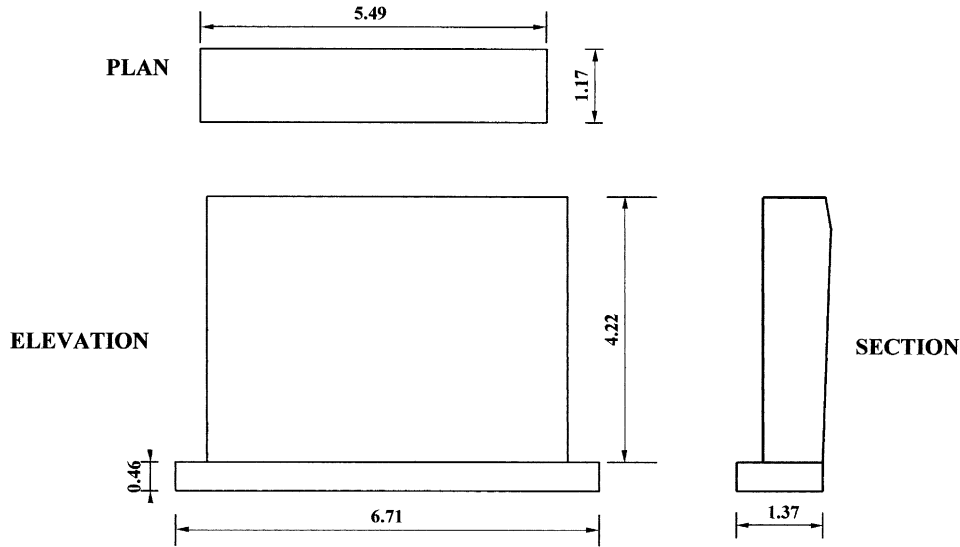


Fig. 3. Abutment of the East Logansport Bridge.

Matthewson et al. [1], recommended that the resultant rotational stiffness for the abutments, can be determined from:

$$K_R = 0.072E_sBH^2 \quad (2)$$

where H is the height of the wall and B is the width of the wall as shown in Fig. 4. Eqs. (1) and (2) are based on the earth pressure distribution against walls subjected to displacement and rotation about the bottom tip of the wall as shown in Fig. 5 [1]. In Figs. 4 and 5, notice that the resultant forces F_1 and F_2 act at distances $0.37H$ and $0.6H$ from the bottom tip of the abutment for the translational and the rotational movements, respectively. Forces F_1 and F_2 have been substituted with a statically equivalent force, F_b , and moment, M_b , acting at the bottom of the abutment. The force displacement equation for the equivalent system is given by:

$$\begin{Bmatrix} F_b \\ M_b \end{Bmatrix} = \begin{bmatrix} K_s & h_1K_s \\ h_1K_s & h_1^2K_s + K_R \end{bmatrix} \begin{Bmatrix} \delta_b \\ \theta \end{Bmatrix} \quad (3)$$

Table 1
Shape factor for abutment stiffness

[L/B]	Shape factor [1]
1	0.80
5	1.70
10	2.00
20	2.40

L : dimension, long side of contact area; B : dimension, short side of contact area.

The stiffness of the foundations at the abutments can be expressed as [20]

$$K = \alpha[K_0] \quad (4)$$

where K_0 is the stiffness matrix of an equivalent circular surface foundation and α is the correction factor. The foundation correction factor can be determined from Fig. 6 [20]. The off-diagonal terms of the stiffness matrix $[K_0]$ can be ignored [6,20]. The coefficients of $[6 \times 6]$ stiffness

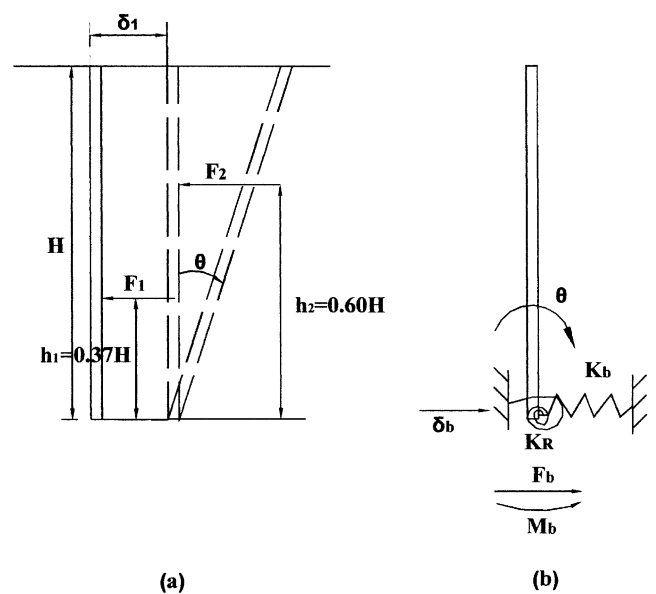
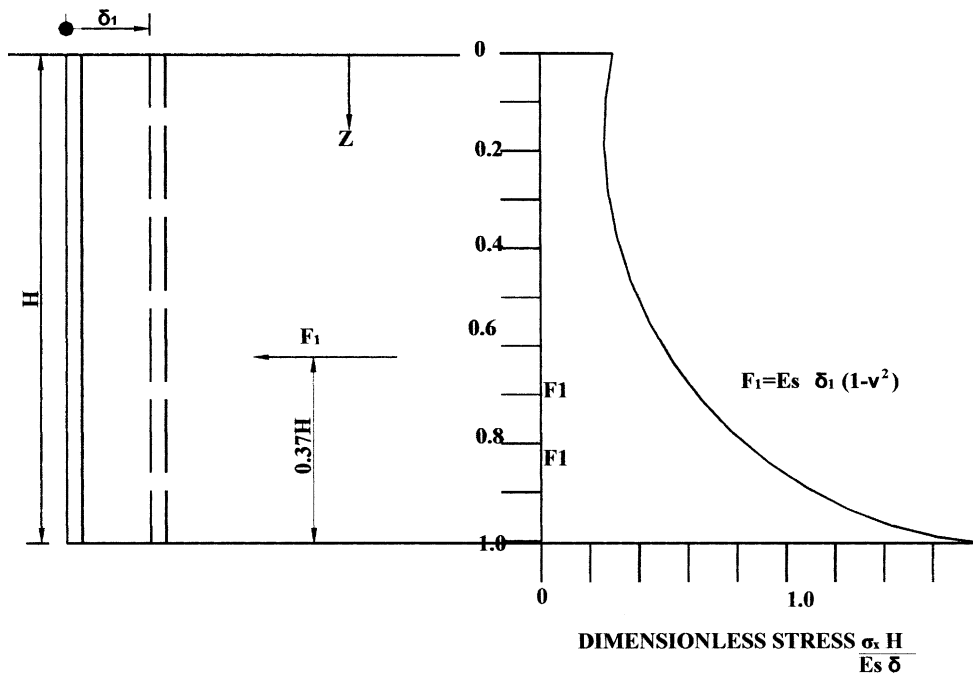
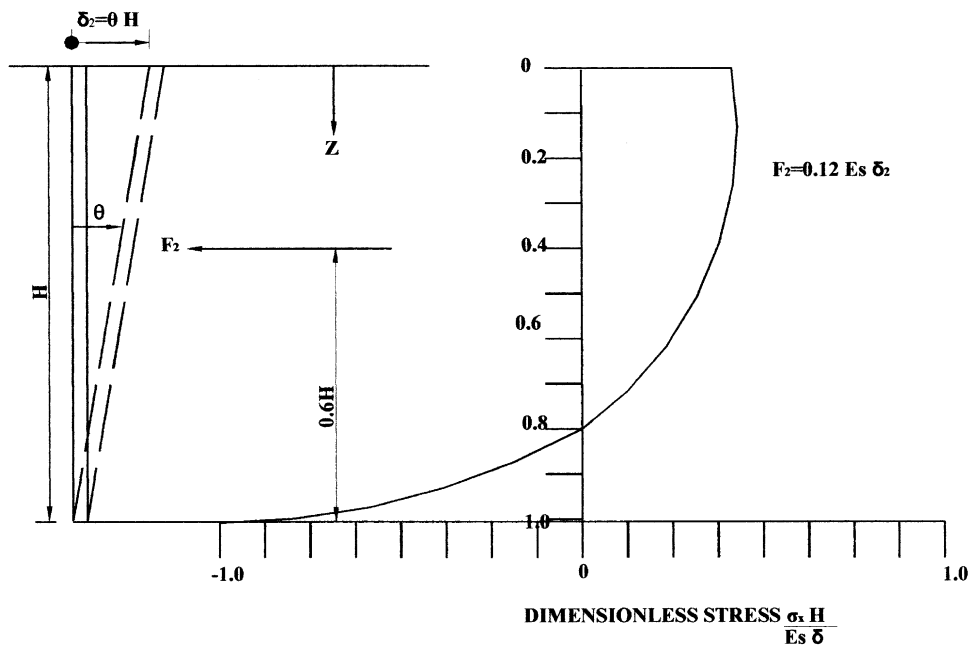


Fig. 4. Abutment–soil model. (a) Forced wall pressure; (b) statically equivalent system.



(a)



(b)

Fig. 5. Wall pressures from forced inward movement (a) wall translated and (b) wall rotated.

matrix $[K_0]$ are expressed by [6,20]:

$$\begin{aligned}
 K_{11} = K_{22} &= \frac{8GR}{2 - \nu} & , K_{33} &= \frac{4GR}{1 - \nu} \\
 K_{66} &= \frac{16GR^3}{3} & , K_{44} = K_{55} &= \frac{8GR^3}{3(1 - \nu)}
 \end{aligned}
 \tag{5}$$

The coefficients K_{44} , K_{55} and K_{66} denote rotational stiffness about the x , y and z axis, respectively, while K_{11} , K_{22} and K_{33} denote translational stiffness along the x , y and z axis, respectively.

For a rectangular foundation with dimensions L , B (see Fig. 6(a)), the radius for the equivalent circular foundation is

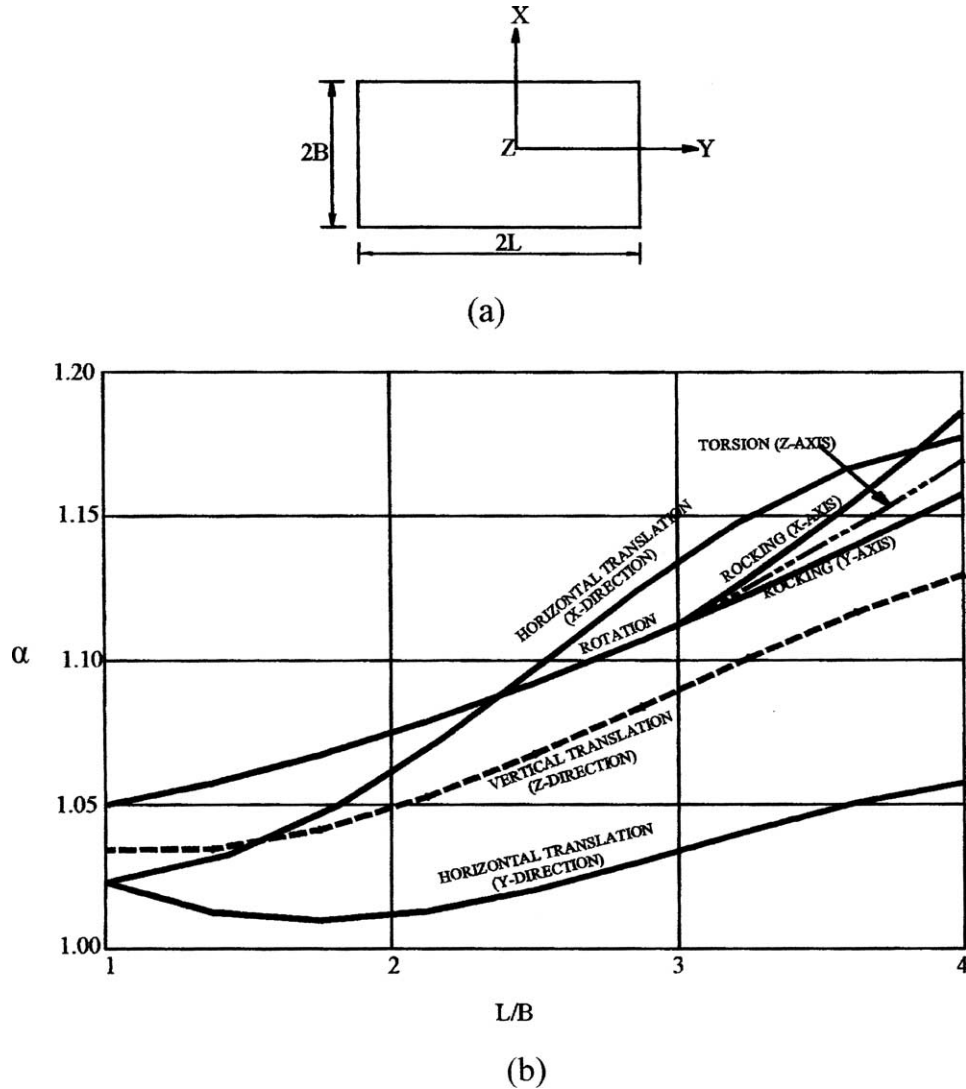


Fig. 6. (a) Rectangular foundation geometry and (b) rectangular foundation correction factor.

given by:

$$R = \sqrt{\frac{4BL}{\pi}}, R_x = \left[\frac{(2B)(2L)^3}{3\pi} \right]^{1/4} \quad (6)$$

$$R_y = \left[\frac{(2L)(2B)^3}{3\pi} \right]^{1/4}, R_z = \left[\frac{4BL(4B^2 + 4L^2)}{6\pi} \right]^{1/4}$$

where R , R_x , R_y and R_z correspond to translational displacement and rocking about the x , y and z axis, respectively. Experimental and analytical studies, e.g. [25], on a single span prestressed-concrete bridge have demonstrated the validity of calculating abutment-wall stiffness and spread footing stiffness based on a linear elastic half-space theory.

Once the abutment wall-backfill stiffness is determined, the second step is the selection of the finite elements that

will be used to model the different parts of the bridge. Although this work addresses issues regarding the dynamic behavior of the bridge, for completeness it is mentioned that for static and thermal loads, the abutments and footings are modeled with eight-node brick elements with three translational degrees-of-freedom per node [11,12]. They are selected among the other element types to describe the behavior of a stiff and bulky part such as an abutment or footing. Plate elements have been selected to model the deck. Six degree-of-freedom beam elements have been used to model the steel tubes. It should be noted that the superstructure of the bridge is post-tensioned with two running longitudinally tendons. In the finite element model, each tendon is modeled with pretensioned cable elements [12], so that they always remain in tension under the applied loads. Such modeling allows consideration of geometric

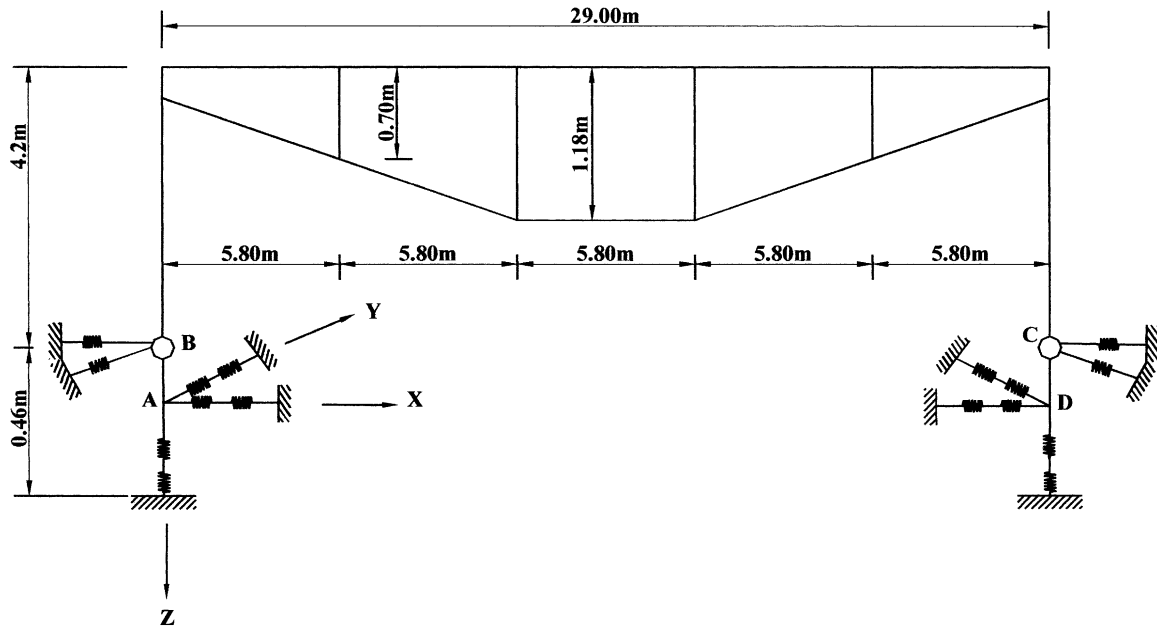


Fig. 7. Frame model for modal and seismic analysis.

stiffness that greatly affects the lower models [12]. Vertical beam elements with large stiffness transfer the forces from the deck to the cables.

3. Modal analysis and sensitivity studies

The steel tubes act as supports of the deck and the concrete panels of the deck are simply placed on the tubes, forming a modular system. Since the concrete panels simply rest on the steel tubes, the cross-section of the deck that resists dynamic loading is only the cross-section of the four tubes. Thus, for dynamic loads the moment of inertia of the deck cross-section is considered to be only the moment of inertia of the four tubes. The contribution of the concrete panels to the deck modeling is limited only to their inertia that is taken into account together with the inertia of the steel tubes.

For dynamic analysis of the post-tensioned system it is also necessary to consider the effect of the axial loading on the deck caused by post-tensioning of the cables. A 3D model using six-degree-of-freedom beam and tension activated cable elements [11,12] is used for the modal and seismic analysis of the bridge, see Fig. 7. In Fig. 7, rotational and translational spring elements are placed at the hinges located at points B and C to simulate the lateral stiffness of the abutments as expressed by Eq. (3). The rotational and translational springs placed at points A and B correspond to the stiffness expressed by Eq. (5).

With the aid of Eqs. (1)–(6), the abutment and foundation soil stiffness can be determined. In order to evaluate the effects of varying the foundation soil properties on the natural frequencies of the structure, a sensitivity study is performed for four types of soil: Type I: rock profile; Type II: deep cohesionless or stiff clay profile; Type III: soft to medium-stiff clay and sand soil profile; Type IV:

Table 2
Foundation stiffness for representative soil types

Spring stiffness	Foundation soil				
	Type IV $G = 3000$ (kPa)	Type IV $G = 14,000$ (kPa)	Type III $G = 24,000$ (kPa)	Type II $G = 70,000$ (kPa)	Type II $G = 275,000$ (kPa)
K_{11} (kN/m)	42436	212179	368440	1060896	4243584
K_{22} (kN/m)	40149	198820	345173	994099	3976395
K_{33} (kN/m)	42436	212179	368440	1060896	4243584
K_{44} (kN m)	375160	1875800	3254400	9390300	37516000
K_{55} (kN m)	368380	1841900	3197900	9209500	36838000
K_{66} (nN m)	38307	190970	332220	957110	3830700

Table 3
Natural frequencies for representative soil types

Frequency (Hz)	Type IV $G = 2758$ (kPa)	Type IV $G = 13790$ (Kpa)	Type III $G = 23788$ (Kpa)	Type II $G = 68950$ (kPa)	Type II $G = 275,800$ (kPa)	Type I rock fixed	Type I rock no backfill
1st	2.13	2.70	2.84 *2.84	2.91	2.97	2.99	2.68
2nd	3.27	3.71	3.82 *3.82	3.92	3.99	4.02	2.99
3rd	3.51	6.50	7.03 *5.60	7.02	7.02	7.02	7.02
4th	4.57	7.02	7.56 *7.10	8.55	8.98	9.13	8.96
5th	7.02	8.12	10.22 *9.91	14.37	16.04	16.40	16.39
6th	8.92	10.52	12.18 *11.83	18.27	25.93	27.26	27.22
7th	14.83	16.45	17.33 *15.40	21.04	34.70	40.47	40.43
8th	19.38	22.44	24.47 *21.49	28.33	38.82	56.24	56.17

soft clay or silt soil profile. The stiffness of the equivalent springs representing the foundation soil are shown in Table 2.

Modal analysis is performed for seven different cases using the spring stiffness shown in Table 2. In the first six cases the backfill spring stiffnesses are taken into account, while in the last case there is no backfill stiffness in the model and the boundary conditions of the soil at the foundation are considered as fixed (rock foundation). Loss of the abutment stiffness refers to the case of extreme displacement at the abutment, i.e. displacement greater than 6 cm caused by seismic loading as suggested in Refs. [3,18], in which case the backfill has failed. The natural frequencies for the East Logansport Bridge are shown in Table 3. In Table 3 the asterisk (*) denotes the value of the frequency when the shear deformation of the beam elements is taken into account. Since the influence of the shear deformation is limited only to the higher frequencies, its effect on the seismic analysis of the bridge is rather insignificant.

The fundamental frequency for $G = 275,800$ kPa, i.e. 2.97 Hz corresponds to the actual foundation of the East Logansport Bridge. This mode is associated with the vertical bending mode of the bridge deck and compares well with the actual bridge fundamental frequency of 2.94 Hz that has been measured experimentally [26]. The difference between the two values is only 1%. The samples have been collected with four strain sensors installed on steel stringers. They have been installed 20.3 cm away from the centerline where the test vehicle would produce the maximum strain. The truck used for testing is a 52000 Tendom, three axle truck with an overall weight of 267.62 kN. Static strains have been measured when the truck passed the bridge at 8 km per hour (crawling speed) and the dynamic strain has been measured at 40 km per hour. The natural frequencies are obtained by analyzing the dynamic response using the signal processing software DADISP [27]. The dynamic response is converted from time domain to frequency domain by performing a Fast Fourier Transformation. Considering all the approximations and simplified assumptions that have been made, the small difference between the measured and the computed

response demonstrates the validity of the finite element model.

In order to assess the influence of the soil type on the bridge modes, as well as the presence of backfill at the abutments, the first four mode shapes are plotted in Fig. 8. Although the natural frequencies depend on the foundation soil type, as shown in Table 3, the corresponding mode shapes have the same configuration for all the examined cases. From Table 3 it can be observed, that the foundation–soil interaction effects on the response characteristics are

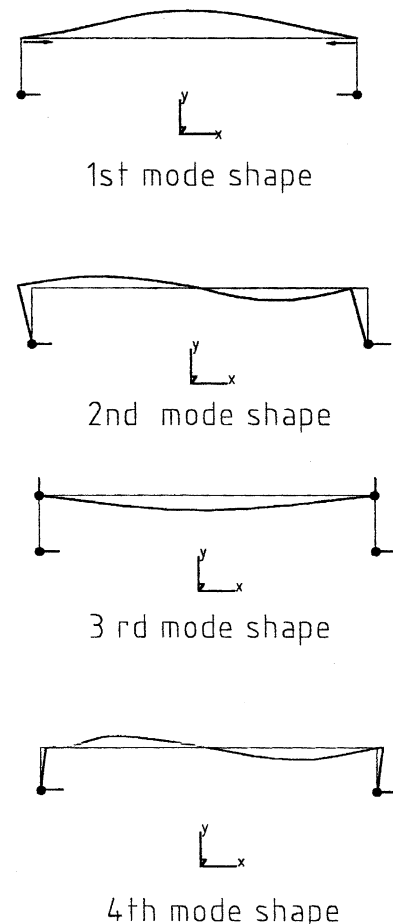


Fig. 8. Mode shapes of bridge model (backfill included).

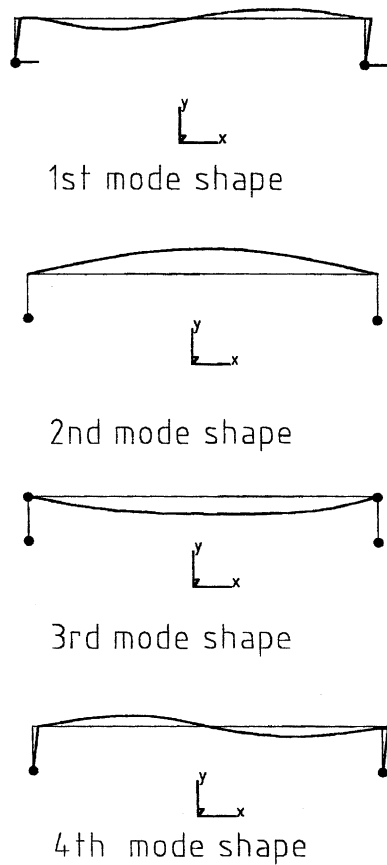


Fig. 9. Mode shapes of bridge model (without backfill).

more significant at the higher modes than at the lower modes. The fundamental frequency of the bridge changed about 40%, between the softest and stiffest foundation soil types. Regarding the other soil types, the fundamental frequency changes even less than 10%. However, for higher modes, the natural frequencies are more sensitive to stiffness variation. As shown in Table 3, the second frequency is less sensitive than the fundamental to soil variation. At the extreme cases of the softest and stiffest soil types, the second mode changes only by about 20%. In view of these observations, it can be concluded that the foundation stiffness does not affect significantly the seismic response of the particular bridge since, as it is shown in Section 4, the mode that contributes the most to the seismic analysis is primarily the second one.

Results presented so far include the combined stiffness of the abutment backfill and the foundation soil. In order to examine the influence of the backfill stiffness on the dynamic characteristics of the bridge the natural frequencies and mode shapes of the bridge are determined ignoring the backfill stiffness. The results are given in column (7) of Table 3. The first four mode shapes of the bridge without backfill are shown in Fig. 9. As shown in Table 3 and Fig. 9, lack of backfill affects the abutment response. Specifically, it changes the fundamental and the second mode, while it has no effect on the vertical modes. This observation is of

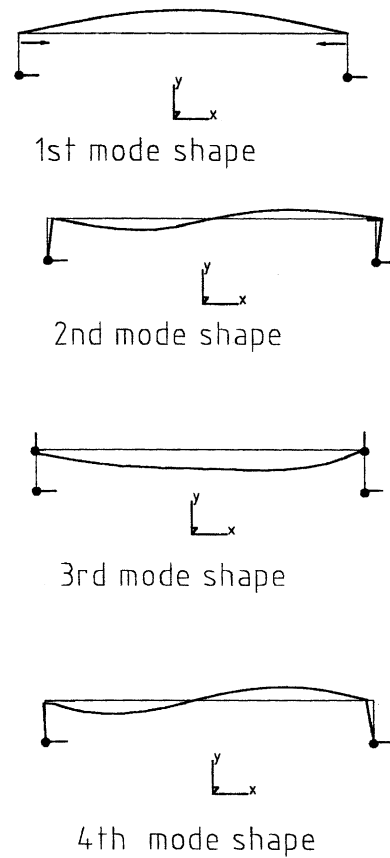


Fig. 10. Mode shapes of the actual East Logansport Bridge model.

great significance because, as it is shown in the following, the seismic behavior of the bridge is determined primarily by the second mode (Fig. 10). Thus, the existence of backfill plays a significant role on the dynamic characteristics and response of the bridge.

4. Seismic analysis and sensitivity studies of the East Longansport Bridge

In order to assess the effects of foundation stiffness on the seismic response of the post-tensioned integral bridge, a sensitivity study is conducted. As shown in Table 4, a total of four foundation soil types have been selected for the sensitivity study. The soil types range from a very soft clay to a rock foundation.

The FHWA/AASHTO design response spectrum at 5% damping, scaled to a peak acceleration of 0.3 g was used for the earthquake loading. Three types of spectra have been recommended in FHWA/AASHTO guidelines for soil types I through IV.

To account for the multi-directional shaking, calculations are conducted for earthquake loading in two orthogonal horizontal (longitudinal and transverse) directions. The two load cases for the seismic analysis are: (a) Load case I: 1.0 Longitudinal + 0.3 Transverse loadings,

Table 4
Maximum displacement on the deck for seismic load cases

Load case	Displacements (cm)					
	Type IV $G = 3000$ (kPa)	Type IV $G = 14,000$ (kPa)	Type $\eta EI G = 24,000$ (kPa) backfill	Type H $G = 70,000$	Type $\eta EI G = 275,000$ (kPa)	Type I rock (kPa) No
I	$D_x = 0.42$	$D_x = 0.39$	$D_x = 0.46$	$D_x = 0.42$	$D_x = 0.39$	$D_x = 0.89$
	$D_y = 0.30$	$D_y = 0.28$	$D_y = 0.34$	$D_y = 0.33$	$D_y = 0.33$	$D_y = 0.61$
	$D_z = 0.03$	$D_z = 0.03$	$D_z = 0.04$	$D_z = 0.04$	$D_z = 0.04$	$D_z = 0.03$
II	$D_x = 0.13$	$D_x = 0.12$	$D_x = 0.14$	$D_x = 0.12$	$D_x = 0.12$	$D_x = 0.22$
	$D_y = 0.09$	$D_y = 0.08$	$D_y = 0.10$	$D_y = 0.10$	$D_y = 0.10$	$D_y = 0.19$
	$D_z = 0.11$	$D_z = 0.09$	$D_z = 0.12$	$D_z = 0.12$	$D_z = 0.11$	$D_z = 0.11$

and (b) Load case II: 0.3 Longitudinal + 1.0 Transverse loadings. The modal response of the East Logansport Bridge is shown in Fig. 8 for the actual soil condition.

Figs. 11 and 12 shows the response of the bridge system for the two load cases for the actual soil conditions of the East Logansport Bridge. For the other soil types the results for load cases I and II are shown in Table 4.

Table 4 shows the effect of varying the foundation stiffness on the displacements of the deck, where D_x, D_y, D_z denote the maximum displacements on the deck along the

axis shown in Figs. 11 and 12. The results clearly indicate that the maximum system response is exhibited for the soil Type III. Also, for a foundation founded on rock without abutment backfill, as shown in Table 4, the maximum displacements are almost double compared to the corresponding ones for the case of a foundation on rock with backfill ($G = 275,000$ kPa). This behavior clearly indicates that the effect of the abutment backfill is very significant to the seismic analysis of the bridge system, exhibiting its worst behavior when the soil is Type III.

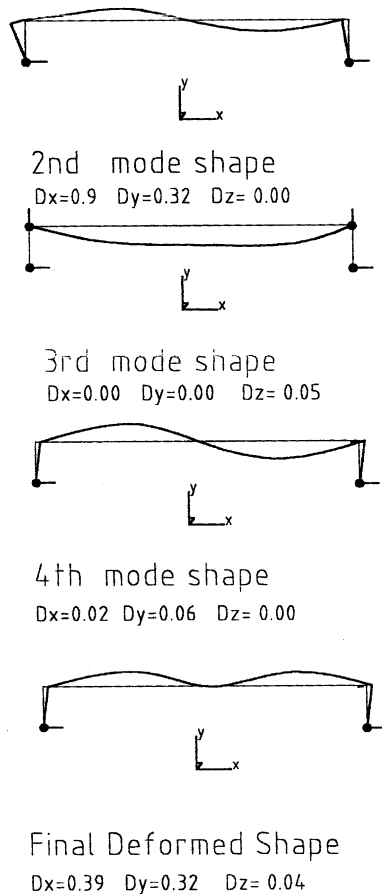


Fig. 11. Response of the East Logansport Bridge (load case I).

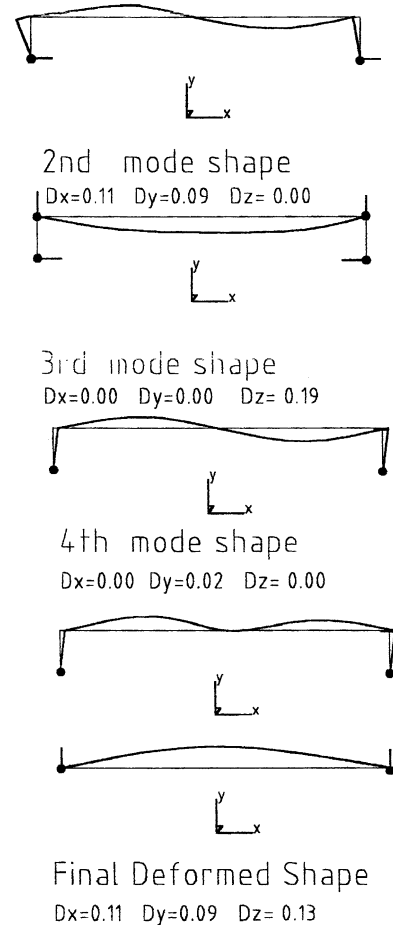


Fig. 12. Response of The East Logansport Bridge (load case II).

5. Conclusions

This study demonstrates the significant role that SSI plays on the dynamic and seismic behavior of integral abutment bridges. This role is of great importance for the post-tensioned modular integral bridge system examined in this study, as depending on soil properties, it could dramatically affect its response to dynamic loads.

The use of easily implemented nondestructive techniques is also demonstrated as a means to develop validated analytical models. Such a validated model has been developed and used to study the seismic behavior of the system for varying soil conditions. The results clearly demonstrate the effect of the backfill on the innovative bridge system.

Additional advantages of the system include the construction of hinges at the foundation abutment joints, as shown in Fig. 3. These joints greatly reduce the effect of thermal loads, creep and shrinkage on the structure, while they also reduce the magnitude of the lateral loads on the foundations.

References

- [1] Matthewson MB, Wood JB, Berril JB. Seismic design of bridges; Section 9: earth retaining structures. Bull N Z Natl Soc Earthquake Engng 1980;13(3):3.
- [2] AASHTO, Guide specifications for seismic design of highway bridges. Highway Subcommittee on Bridges and Structures; 1983.
- [3] Eurocode 8, Part 2—Bridges, ENV; 1988-2.
- [4] Imbsen RA. Seismic design of highway bridges. Workshop Manual, Report No. FHWA-IP-81-2; 1981.
- [5] Wolf JP. Dynamic soil–structure interaction. ; 1985. Englewood Cliffs, NJ.
- [6] Antes H, Spyarakos CC. Soil–structure interaction. Computer analysis and design of earthquake resistant structures: a handbook; 1997. Chapter 6, p. 271–332.
- [7] Spyarakos CC. Assessment of SSI on the longitudinal seismic response of short span bridges. Engng Struct 1990;12:60–6.
- [8] Spyarakos CC. Seismic behavior of bridge piers including soil–structure interaction. Comput Struct 1992;4(2):373–84.
- [9] Crouse CB, Hushmand B, Martin GR. Dynamic soil–structure interaction of a single-span bridge. Earthquake Engng Struct Dyn 1987;15:711–29.
- [10] Levine MB, Scott RF. Dynamic response verification of simplified bridge foundation model, I. J Geotech Engng 1989;15(2):1246–61.
- [11] Priestley MNJ, Seible F, Calvi GM. Seismic design and retrofit of bridges. New York: Wiley; 1996.
- [12] Spyarakos CC. Finite element modeling in engineering practice. PA, USA: Algor Publishing Division; 1995.
- [13] Saidi M, Douglas BM. Effect of design seismic loads on a highway bridge. J Struct Engng 1984;110(11).
- [14] Wilson JC. Stiffness of non-skew monolithic bridge abutments for seismic analysis. Earthquake Engng Struct Dyn 1988;16:867–83.
- [15] Maragakis EA. Elastic stiffness of flared bridge columns with foundation springs. J Struct Engng 1986;112(8).
- [16] Ellassaly M, Ghali A, Elbadry M. Influence of soil conditions on the seismic behavior of two cable-stayed bridges. Can J Civil Engng 1995;22:1021–40.
- [17] Cook TL, Burdette EG, Graves RL, Goodpasture DW, Deathrage JH. Effect of varying foundation stiffness on seismically induced loads in bridge bents: a sensitivity study. Transportation research record 1476, Washington, DC: Transportation Research Board, National Research Council, National Academy Press; 1995. p. 84–97.
- [18] Karantzakis M, Spyarakos CC. Seismic analysis of bridges including soil–abutment interaction. Proceedings of the 12th World Congress on Earthquake Engineering. Paper No. 2471, New Zealand; 2000.
- [19] Vlassis AG, Spyarakos CC. Seismically isolated bridge piers on shallow soil stratum with soil–structure interaction. Comput Struct 2001;79:2847–61.
- [20] Earth Technology Corporation. Seismic Design of Highway Bridge foundations. Volumes II and III, Report No. FHWA/RD-86/103, US Department of Transportation; 1986.
- [21] Crouse CB, Hushmand B, Martin G, Liang G, Wood J. Dynamic response of bridge–abutment–backfill systems. Paper presented at the joint US–New Zealand Workshop on Seismic Resistance of Highway Bridges, San Diego, CA; May 8–10 1985.
- [22] Seismic Specifications for Bridge Design. Greek Ministry of Construction, December; 1999.
- [23] Lam IP, Martin R, Imbsen R. Modeling bridge foundations for seismic design and retrofitting. Transport Res Record 1991;1290:113–26.
- [24] Poulos HG, Davis EH. Elastic solutions for soil and rock mechanics. New York: Wiley; 1974.
- [25] Crouse CB, Hushmand B, Martin J. Dynamic soil–structure interaction of a single-span bridge. Earthquake Engng Struct Dyn 1987;15:711–29.
- [26] Spyarakos CC. Dynamic load factor in composite highway bridges. Proceedings of Structures Under Shock and Highway Impact V, Computational Mechanics Publication; 1998. p. 211–20.
- [27] DADISP Software. DSP Development Corporation. One Kendall Square, Cambridge, MA 02139.